Characterising patterns of turbulent heat exchange over snow in an alpine ski area with infrared camera

Heather Purdie, Marwan Katurji, Rajasweta Datta, Peyman Zawar-Reza
Department of Geography, University of Canterbury, Christchurch, New Zealand

1. Introduction

The snow surface temperature distribution in alpine catchments influences snowpack metamorphism and stability. Temperature gradients between the snow surface and the underlying layers produce water vapour gradients within and between snow crystals. These processes change the shape and bonding of snow crystals which can strengthen a snowpack, but can also create weak layers if the temperature gradient exceeds a critical threshold (McClung and Scharer, 2006). From a snowmelt perspective, better understanding of how snow surface temperature varies spatially will improve meltwater estimates derived from surface energy balance models, which often assume the snow surface temperature is 0°C (Hock, 2005). However, Cullen & Conway(2015) note that even in summer, there are times when the snow surface temperature does not reach melting point.

From a radiative perspective snow surfaces are complex; characterised by high albedo, high emissivity, low thermal admittance, and transmission of short-wave radiation (Oke, 1987). It is the high emissivity and low thermal admittance that makes snow an ideal yet challenging medium for infrared (IR) thermography. Snow behaves almost as a full radiator, with an emissivity of ~0.98-0.99 (Kinar and Pomeroy, 2015), and the low thermal admittance of snow means that rapid changes of surface-layer air temperature register as fluctuations in brightness temperature at the interface between snow and air.

The application of thermography to cryosphere science has been reviewed by Kinar and Pomeroy (2015), with more recent studies focusing on snowpit analysis (Shea et al., 2012; Schirmer and Jamieson, 2014) and analysis of glacier surface temperature (Aubry-Wake et al., 2015). Shea and Jamieson (2011) also highlight fundamental principles and limitations in their exploration of snow surface temperatures. There is much to learn about thermography and its application to snow and ice research.

Here we examine the feasibility of deriving spatial and temporal changes in snow surface temperatures that can influence snow stability and meltwater production. We hypothesise that surface temperature variability is mainly controlled by the sensible heat exchange between the snow surface and the atmosphere, and by using Time-Sequential Thermography (TST) we aim to understand this variability. TST involves acquiring broadband IR images of the surface from a fixed-platform at a high sampling rate (0.1Hz), to subsequently deduce pixel-scale statistics of brightness temperature. Pixel-scale statistics help to shed light on the turbulent nature of the atmosphere which drives the sensible heat flux and controls the snow surface temperature.

2. Methods:

Study site

Our study site was a small snow-slope within an alpine ski basin, located in the Canterbury high-country (Fig 1). We selected a snow slope that contained a mixture of smooth and textured snow surfaces, small topographic depressions, and some exposed rocks and vegetation (Fig 1). The heterogenetic surface was purposeful to enable assessment of how brightness temperature varies with micro-topography. The IR camera was set-up on a flat section at a break in the slope with an average photographic angle of 25° for the near-target (≤30 m) elements and 30° for elements 20-200 m. Within the field-of-view (FOV) we inserted into the snow two poles with regularly spaced thermistors to measure subsurface temperatures. These poles were pushed right through the snowpack so that the bottom-most thermistor was positioned 5cm above the ground. The lower and upper poles were 6 and 21 m from the camera respectively. An automatic weather station with sensors for surface temperature, wind speed and wind direction was installed further up the slope 28 m distant. The overall slope aspect was southeast (Fig 1 and Table 1).

Data Analysis

We follow the spatio-temporal decomposition methods of Christen et al. (2012) to separate mean patterns and trends from high-frequency fluctuations (see Table 2 Christen et al., 2012). To further consider spatial patterns, polygons were digitised around different surface types enabling extraction of average values. Variability between adjacent pixels could range to from 0.04-0.13°, so extracting average pixel values from the polygons provided a robust way to compare surface types.

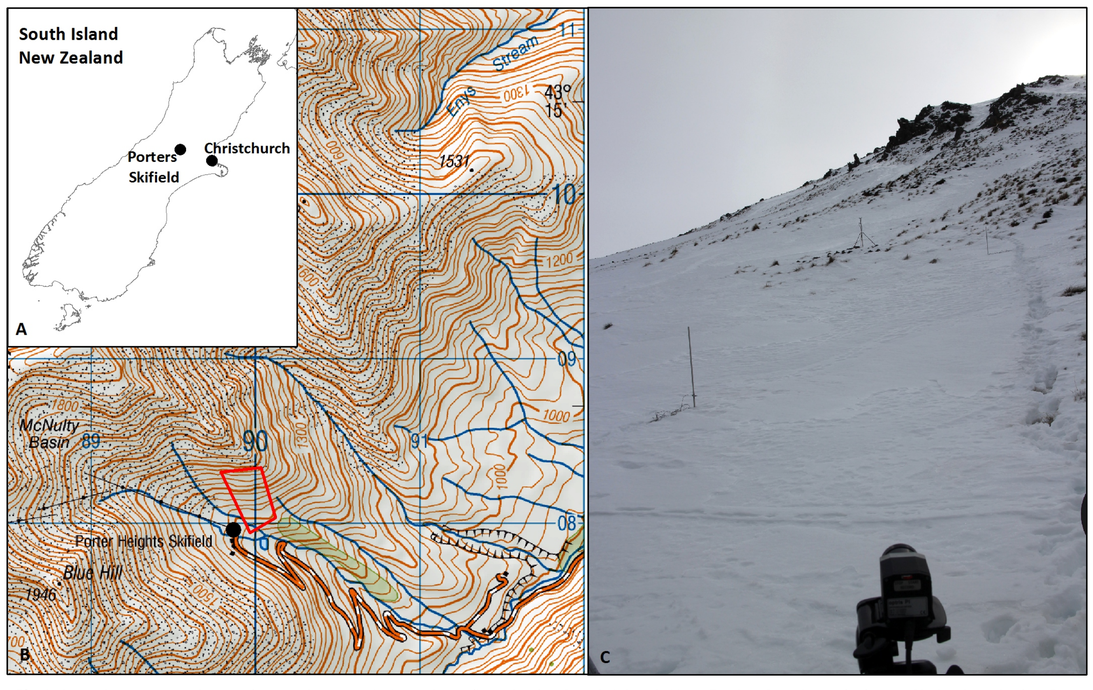

Fig 1: Location map and experimental setup. A: Location of study site South Island, New Zealand and proximity to Christchurch city. B: Porters skifield showing access road and elevation contours. The red box indicates area used in the study. C: Experimental setup showing camera, automatic weather station and poles with Hobo sensors driven into the snow.

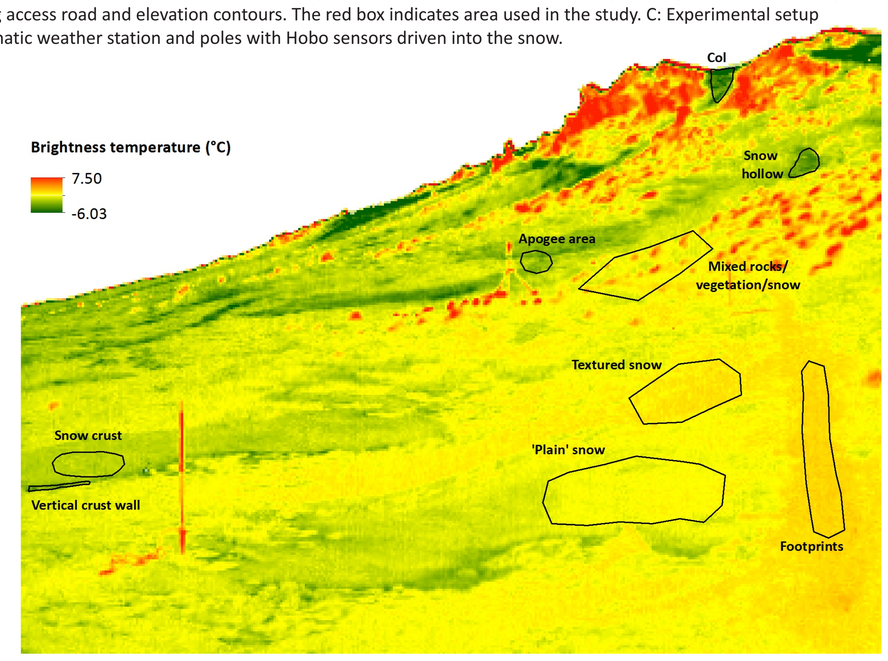

Fig 3: Brightness temperatures for an instantaneous image (*fpattern*) taken at 12:20 showing warmer/cooler regions and polygons used to derive averages for different surface types.

Table 1: Instrumentation specifications and measured variables

Instrument	Description	Measured Variable	Range and Accuracy	Sampling Frequency
Optris pi450	Uncooled infrared camera	Brightness temperature on raster of 288x382 pixels	-20 to 900°C ±2°C Spectral range 7.5 to 13µm Thermal sensitivity 40mK	0.1 Hz
Apogee S1-111	Infrared radiometric	Target temperature	±0.2 °C Spectral range 8-14 µm	0.1Hz
Young 8500 2D anemometer	Sonic anemometer	Wind speed Wind direction	±0.1 ms^{-1} ±3°	0.1 Hz
Hobo H08-030-08	Thermistor	Temperature	±0.3°C	0.1 Hz

3a. Results & Discussion

Temporal variability

Comparison of data recorded by the Apogee and the spatially averaged Optris data for the same areas in an instantaneous image showed initially (12:20) the two instruments were within 0.02 °C. However over time, the two data sets diverge (Fig 2), and there was no significant statistical correlation between the two data sets. Post-processing demonstrated that the warming trend in the Optris data was in-part due to instrument warming (see later). A negative linear relationship was found between wind-speed and the Apogee snow surface temperature (Pearson's r= -0.517, p=0.00), but no relationship was found between wind-speed and the Optris data (both raw and post-processed).

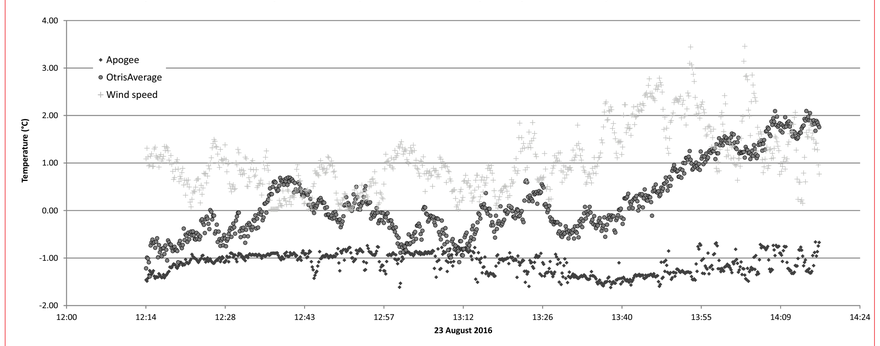

Fig 2: Snow surface temperature recorded by the Apogee and Optris plotted with wind-speed over time.

Spatial variability

Temperature comparison of spatially separated pixels in an instantaneous image (*fpattern*) revealed coldest surface temperatures in depressions (-1.93°C) and in higher elevation cols (-2.85°C). Smooth, undisturbed snow surfaces (crust layer) were ~1.3°C cooler than textured snow surfaces (e.g. surfaces exhibiting small-scale scalloping from wind transport). Highly disturbed surfaces (e.g. footprints) were 0.8°C warmer then adjacent undisturbed snow, and 1.7 °C warmer than smooth crust surfaces (Fig 3).

The colder temperatures recorded in topographic depressions may be attributed to cold air pooling and a lack of turbulence, but may also be related to micro-aspect and sky view, which were not able to be assessed here. We attribute the colder pixel temperatures of the smooth surfaces to more efficient reflection of short wave radiation from specular (as opposed to diffuse) scattering. The warmer pixel temperature recorded in the region disturbed by footprints was unexpected, and we can only speculate possible explanations without further experiment. Increased surface roughness associated with the footprints may result in a complicated pattern of heat emission due to large variability in micro-scale aspect trapping heat within the disturbed snow surface.

Analysis of *mpattern* showed the spatial patterns identified in Fig 3 persisted over the entire time sequence.

Spatiotemporal variability

mtrend is defined as the "departure of the average temperature of an instantaneous image from the spatiotemporal average of the time sequence" Christen et al. (2012, p306), and that subtraction of *mtrend* can help reduce sensor drift. Removal of *mtrend* from the time-series does reveal differences in spatiotemporal variability between the different surface types (Figs 3 & 4).

Locations further upslope record larger changes in brightness temperature over time compared to locations lower and closer to the camera. The drop in temperature recorded near the apogee and in the snow hollow at 12:37 and 13:10 coincided with changes in wind direction to east and southeast flows. Conversely the distinctive jump in temperature at 13:22 and general warming trend after 13:30 coincide with wind from a north-westerly direction. It is possible that these sites were more exposed to changes in wind direction than the lower-angled slopes near the camera.

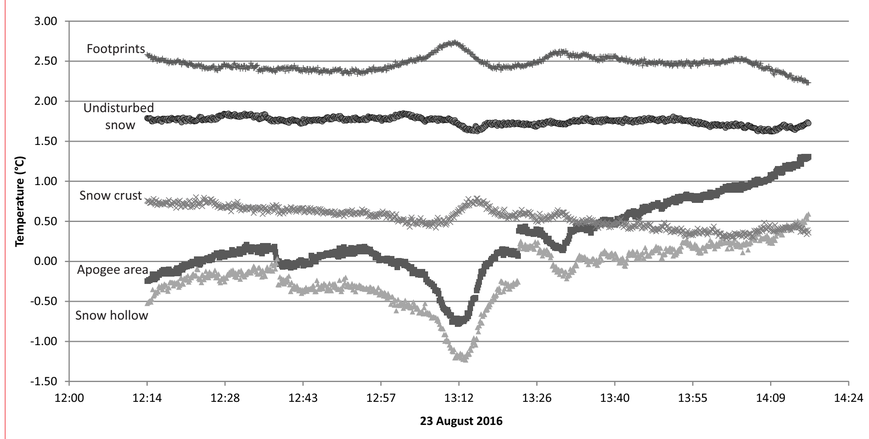

Fig 4: Detrended time series for different surface types, showing locations further upslope reacting differently than regions 10 m lower and 20 m closer on the slope.

3b. Results & Discussion continued

Relationship with sub-surface temperature

20 cm and more below the surface, the snowpack was isothermal at 0.16 °C (Fig 5). Sensors near the snow surface (-2 and -15 cm depth) showed a step-wise warming trend over time (Fig 5). Internal transmission of radiation through snow can be problematic and it is possible this warming is a result of thermistor warming, i.e. the sensor recording its own temperature response and not that of the surrounding snowpack (Oke, 1987, p85). This limits our interpretation of potential thermal gradients. Even so, the large spatial variability in snow surface temperature recorded by the IR camera indicates that temperature gradients will vary in magnitude across space and time.

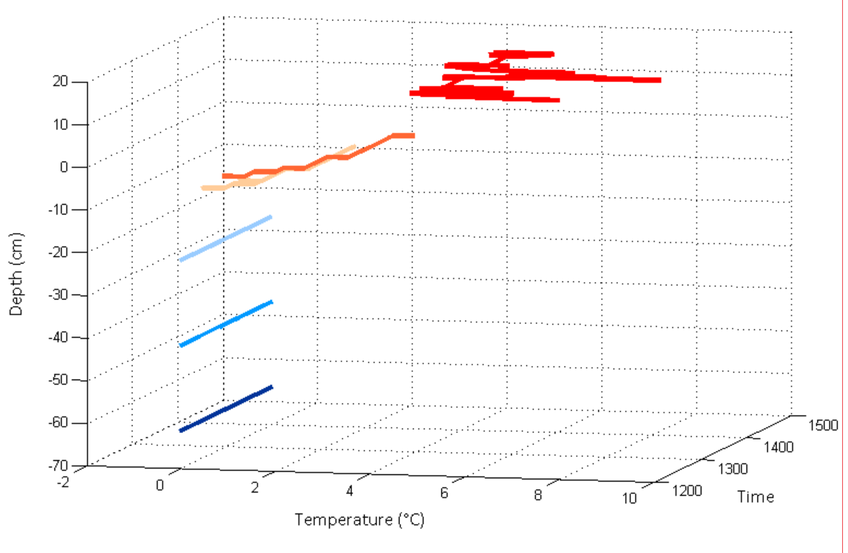

Fig 5: Change in snow temperature with depth over time as recorded at the Hobo snow-pole

3c. Results & Discussion continued

Pixel-scale variability

The standard deviation of *ftotal* is used to reveal any instrument effects, and Fig 6 does show an imprint of the microbolometer. However, this variability only accounts for 0.04-0.15°C, which in consideration of the actual camera error (2°C) is minimal. Taken over the entire time sequence (*stdftotal*) this background noise amounts to around 0.07°C.

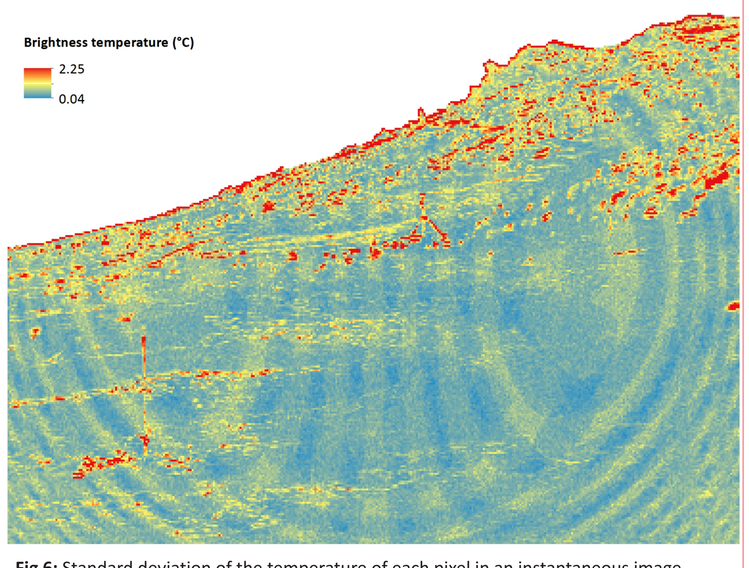

Fig 6: Standard deviation of the temperature of each pixel in an instantaneous image

Cloud cover and micro-aspect

At the start of our experiment sky conditions were blue-sky with patchy cloud cover. This meant that there was variability in sun-shadow with cloud movement. The overall southeast aspect of the slope meant that early in the experiment there was some shadow being created by small-scale relief features (e.g. grass, rocks) as the sun shone across the slope. This effect disappeared over time due to increasing cloud cover and the sun tracking northwards. Once the northwest flow established there was almost complete cloud cover. Changes in cloud cover in combination with micro-aspect and heterogeneous snow crystal orientation are expected to influence brightness temperature, the effects of which cannot be accounted for here but warrants further investigation.

4. Conclusions

TST has the potential to further knowledge about energy snowpack exchange at very high spatiotemporal resolution. However, high variability in snow crystal orientation, micro-topography and general alpine climatology means much care is needed with experimental design and data interpretation. Large spatial variability in snow surface temperatures identified between different locations within our study area demonstrates that even within a relatively small ski basin, temperature gradients and snowpack evolution will be complex.

Considerations for future research:

1. Micro-scale studies utilising two matching IR cameras and radiometric infrared temperature sensors to better understand how brightness temperature is affected by small-scale slope aspect complexity and sky view factors.
2. Obtain and utilise high resolution digital elevation models (e.g. LIDAR) to improve links between changes in brightness temperature and micro-topography.
3. Improve general field set-up to include the use of 'perfect' diffuse reflectors e.g. Shea and Jamieson (2011), and well-insulated sub-surface temperature sensors at higher spatial resolution e.g. ≤5cm depths.

References

Aubry-Wake, C. et al., 2015. Measuring glacier surface temperatures with ground-based thermal infrared imaging. Geophysical Research Letters, 42: 8489-8497.

Christen, A., Meier, F. and Scherer, D., 2012. High-frequency fluctuations of surface temperatures in an urban environment. Theoretical and Applied Climatology, 108: 301-324.

Cullen, N.J. and Conway, J.P., 2015. A 22 month record of surface meteorology and energy balance from the ablaiton zone of Brewster Glacier, New Zealand. Journal of Glaciology, 61(229): 931-946.

Hock, R., 2005. Glacier melt: a review of processes and their modelling. Progress in Physical Geography, 29(3): 362-391.

Kinar, N.J. and Pomeroy, J.W., 2015. Measurement of the physical propertities of the snowpack. Reviews of Geophysics, 53: 481-544.

McClung, D. and Schaerer, P., 2006. The Avalanche Handbook. The Mountaineers Books, Seattle.

Oke, T.R., 1987. Boundary layer climates. Taylor and Francis, London.

Schirmer, M. and Jamieson, B., 2014. Limitations of using a thermal imager for snow pit temperatures. The Cryosphere, 8: 387-394.

Shea, C. and Jamieson, B., 2011. Some fundamentals of handheld snow surface thermography. The Cryosphere(5): 55-66.

Shea, C., Jamieson, B. and Birkland, K.W., 2012. Use of thermal imager for snow pit temperatures. The Cryosphere, 6: 287-299.

We would like to acknowledge the ongoing support of Porters ski field and staff Simon Morris for permission and assistance with field work. Also Paul Bealing, Justin Harrison, Rasool Porhemmat for assistance with field and/or data anaylsis.

Questions or feedback contact Heather at heather.purdie@canterbury.ac.nz

UNIVERSITY OF CANTERBURY
Te Whare Wānanga o Waitaha
CHRISTCHURCH NEW ZEALAND